A&A 500, 827–831 (2009)
DOI: 10.1051/0004-6361/200911785

Astronomy & Astrophysics

A high-speed bipolar outflow from the archetypical pulsating star Mira A

J. Meaburn[1], J. A. López[2], P. Boumis[3], M. Lloyd[1], and M. P. Redman[4]

[1] Jodrell Bank Centre for Astrophysics, University of Manchester, Manchester, M13 9PL, UK
e-mail: jmeaburn@jb.man.ac.uk, Myfanwy.Lloyd@manchester.ac.uk
[2] Instituto de Astronomia, UNAM, Apdo. Postal 877, Ensenada, B.C. 22800, Mexico
e-mail: jal@astrosen.unam.mx
[3] Institute of Astronomy & Astrophysics, National Observatory of Athens, I. Metaxa & V. Pavlou, P. Penteli, 15236 Athens, Greece
e-mail: ptb@astro.noa.gr
[4] Centre for Astronomy, National University of Ireland, Galway, University Road, Galway, Ireland
e-mail: Matt.Redman@nuigalway.ie

Received 4 February 2009 / Accepted 12 March 2009

ABSTRACT

Optical images and high-dispersion spectra have been obtained of the ejected material surrounding the pulsating AGB star Mira A. The two streams of knots on either side of the star, found in far-ultraviolet (FUV) GALEX images, have now been imaged clearly in the light of Hα. Spatially resolved profiles of the same line reveal that the bulk of these knots form a bipolar outflow with radial velocity extremes of $\pm$150 km s^{-1} with respect to the central star. The south stream is approaching and the north stream receding from the observer. A displacement away from Mira A between the position of one of the south-stream knots in the new Hα image and its position in the previous Palomar Observatory Sky Survey (POSS I) red plate was noted. If interpreted as a consequence of expansion proper motions, the bipolar outflow is tilted at 69° $\pm$ 15° to the plane of the sky, has an outflow velocity of 160 $\pm$ 10 km s^{-1} and is $\approx$1000 y old.

Key words. stars: circumstellar matter – stars: variables: general – stars: binaries: general – stars: individual: Mira

1. Introduction

The binary system Mira AB has attracted attention for over 400 yr (for a summary see Hoffleit 1997). Apart from being very close to the Sun (Hipparcos distance of 107 ± 10 pc), Mira A is the archetypical pulsating variable star with a period of hundreds of days and a brightness range of 8 mag (Reid & Goldston 2002). Its periodic outbursts over the last 80 cycles are listed by Percy & Bagby (1999). Hubble Space-telescope images have shown Mira B to be separated by $\approx$0.5″ from A ($\equiv$54 AU; Karovska et al. 1997). Mira A of intermediate mass is certainly in its volatile asymptotic giant branch (AGB) phase, whereas B has been previously identified as a white dwarf but recently as a somewhat innocuous F-type star similar to the Sun though with an accretion disk formed by the mass ejections from A (Karkovska et al. 2005; Ireland et al. 2007, and refs. cited therein). In either case B is too well-separated from A to significantly affect the overall dynamics of the ejected material.

Interest in Mira A has been further heightened by the discovery of a 2° long ($\approx$4 pc) FUV emitting tail with the GALEX satellite (Martin et al. 2007). They propose that this traces the interactions with the local interstellar medium (ISM) over the past 30 000 y of the ejected material from Mira A. This is plausible (Wareing et al. 2007), because the star has a high space velocity of 120 km s^{-1} at an angle of 28° with respect to the plane of the sky, is tilted away from the observer, and has what appears to be a preceding bow-shock (Raga & Canto 2008). Perhaps relevant is the tail of similar dimensions apparently projecting from the similarly mass-ejecting, proto-typical, luminous blue variable (LBV) star P Cygni (Meaburn et al. 1999), although later, deeper observations in the higher excitation [O III]5007 Å line show this tail as part of a larger complex of filaments yet still convincingly associated with the star (Meaburn et al. 2004; Boumis et al. 2006, and references therein).

In the GALEX FUV images a group of emission knots close to Mira AB and called "North Stream" and "South Stream" by Martin et al. (2007) have been identified as recent manifestations of the mass ejections from Mira A. As these are within a field of a few arcmin diameter, they have now been investigated at optical wavelengths using occulting strip imagery, to exclude scattered continuum light from the bright stellar image, and longslit, spatially resolved, high-dispersion spectrometry. The results of these optical observations will now be presented.

2. Observations and results

Observations were made with the Manchester Echelle Spectrometer (MES-SPM – see Meaburn et al. 1984, 2003) combined with the 2.1-m San Pedro Martir, (B.C. Mexico) telescope on 2008 Oct. 26 to 28. A SITe CCD was the detector with 1024 × 1024, 24 μm pixels, although 2 × 2 binning was employed. The "seeing" throughout was $\approx$1″.

2.1. Imagery

MES-SPM has a limited imaging capability with a retractable plane mirror isolating the echelle grating and a clear area (4.37 × 5.32 arcmin^2) replacing the spectrometer slit.

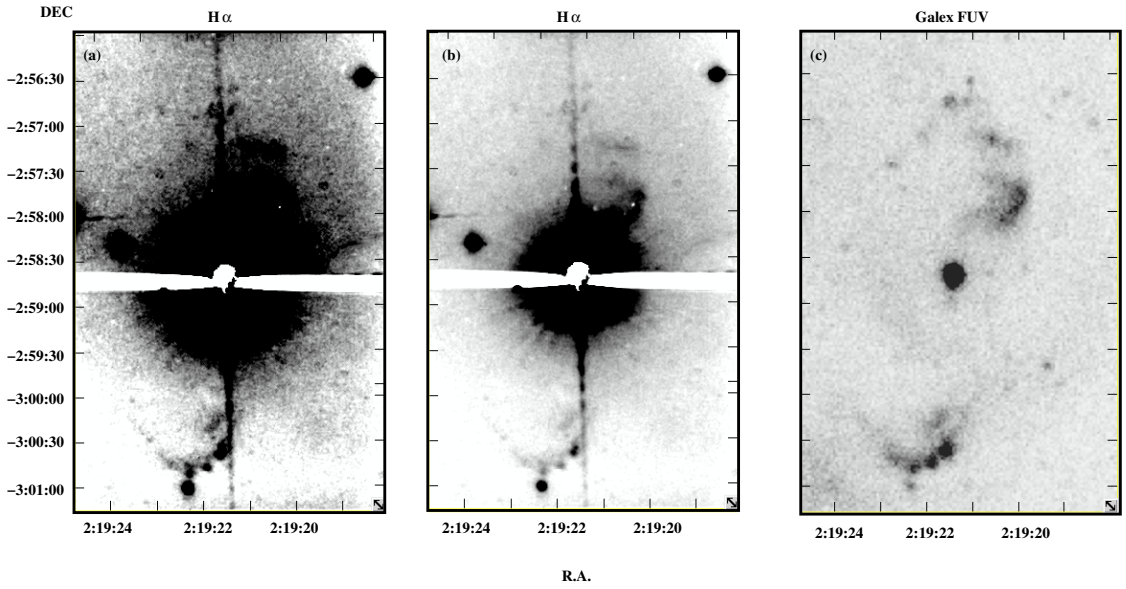

Fig. 1. Deep and lighter representations in panels **a)** and **b)**, respectively, of the new Hα image of the knots obtained on 2008 Oct. 28 and compared in panel **c)** with the FUV image of Martin et al. (2007) obtained on 2006 Nov. 18–Dec. 15. The occulting strip seen in **a)** and **b)** minimizes the scattered light of Mira A within the telescope and instrumental optics. Coordinates throughout are from the 2000 epoch.

The image in Fig. 1 is a subset from this larger field obtained on the 2008 Oct. 28. An occulting strip of chromium suppressed the bright image of Mira. The integration time was 2000 s. The coordinates (J2000) were added using the STARLINK GAIA software. The 90 Å bandwidth interference filter predominantly transmits the Hα nebular line, as [N II] 6548 & 6584 Å emission has been shown (Martin et al. 2007) to be very low. Confusing, faint star images were eliminated using the PATCH routine of the STARLINK GAIA software. Deep and lighter representations of the new Hα image are compared in Fig. 1 to the FUV GALEX image from Martin et al. (2007).

2.2. Longslit spectroscopy

Spatially resolved, longslit Hα line profiles were obtained with the MES-SPM along the lines marked 1–6 in Fig. 2. These are only partial lengths of the full NS slits, because measurable Hα emission only occurred over small sections of the full slit lengths containing the bright knots in the north and south streams. The increments along the slit length each corresponds to 0.63″.

In this spectroscopic mode MES-SPM has no cross-dispersion; consequently, for the present observations, a filter of 90 Å bandwidth was used to isolate the 87th echelle order containing the Hα and [N II] 6548 & 6584 Å nebular emission lines. The slit width was always 300 μm, which is ≡3.8″ on the sky and 20 km s^{-1} spectral halfwidth (HPBW). Each integration time was 1800 s. Also indicated in Fig. 2 are the directions of the 2° long FUV emitting tail detected by Martin et al. (2007) and of the proposed bowshock found in the same wavelength domain.

The longslit spectra were cleaned of cosmic rays, bias corrected, and calibrated in wavelength to ±1 km s^{-1} accuracy in the usual way using STARLINK FIGARO software. The greyscale representation of the position-velocity (pv) arrays of Hα line profiles (after subtraction of the sky background spectra) for the partial slit lengths shown in Fig. 2 for Slits 1–4 and 5–6 are shown in Figs. 3 and 4, respectively. Here contours of the

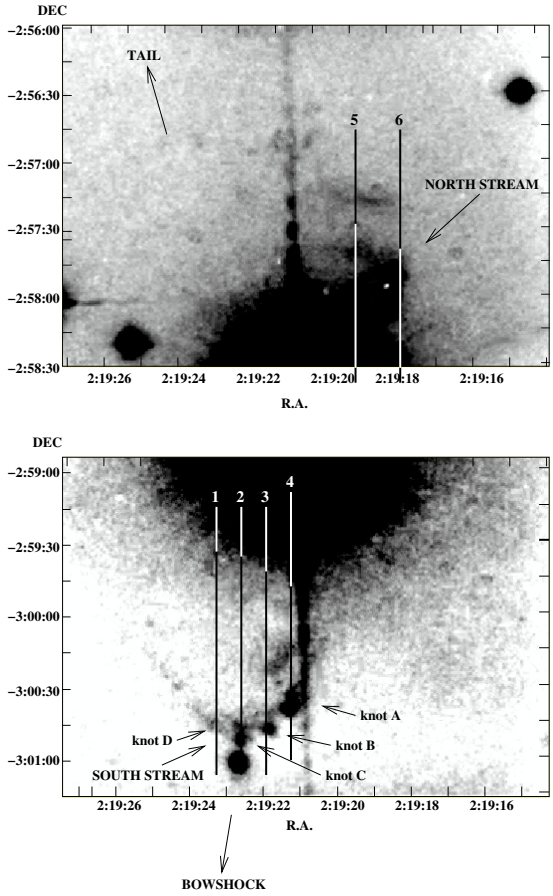

Fig. 2. Parts of the lengths of the spectrometer slits containing useful Hα profiles 1–4 over the southern knots (South Stream) and 5–6 over the northern knots (North Sream). The directions of the FUV tail and bowshock are also indicated. *The top panel* shows the new Hα image in Fig. 1 but printed lightly to show the details of the North Stream and the bottom window is deeper for the South Stream. The relative positions of the two panels in this figure are somewhat arbitary.

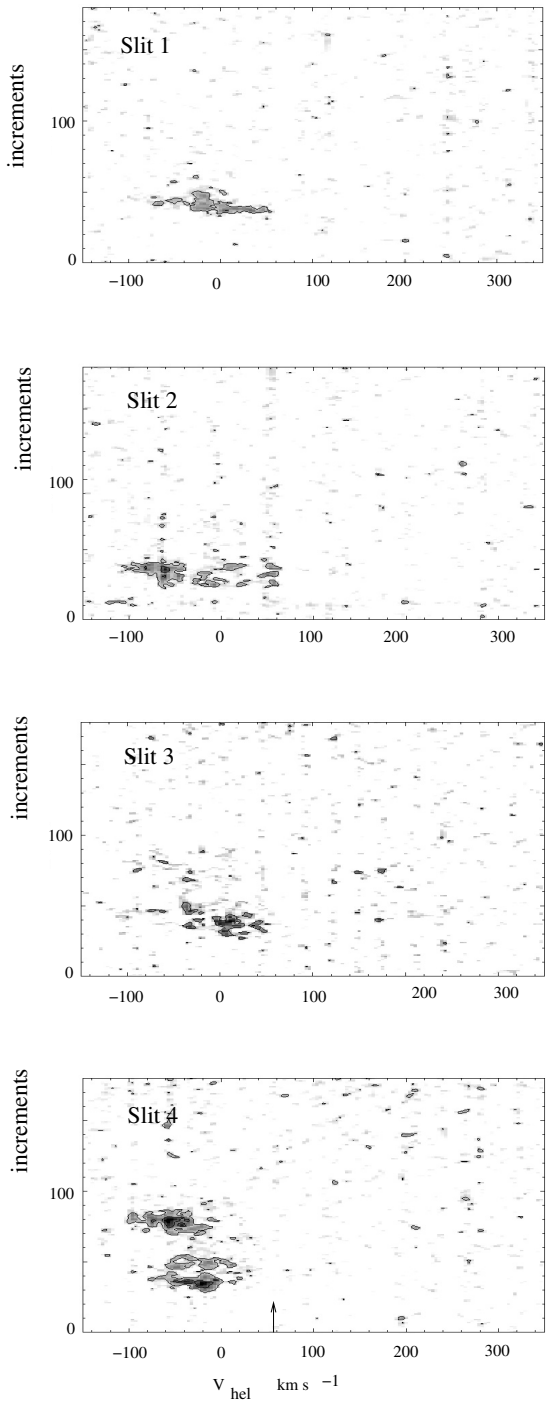

Fig. 3. Contoured and greyscale representations of the pv arrays of Hα line profiles from the South Stream of knots shown in Figs. 1 and 2. These are for the slit lengths 1–4 shown in Fig. 2. The spectra of the background have been subtracted in all cases. The heliocentric systemic radial velocity V_{sys} of Mira A is arrowed. North is to the top of each slit length and each increment is ≡0.63 ″.

Hα relative surface brightnesses with linear intervals have been overlaid on the negative greyscale representations. As no standard star was observed, the absolute surface brightnesses were unreliable and are not presented here. Line profiles from various incremental lengths of these pv arrays of profiles are shown in Fig. 5. As the background spectra have been subtracted in all of these profiles the noise fluctuates around the zero level.

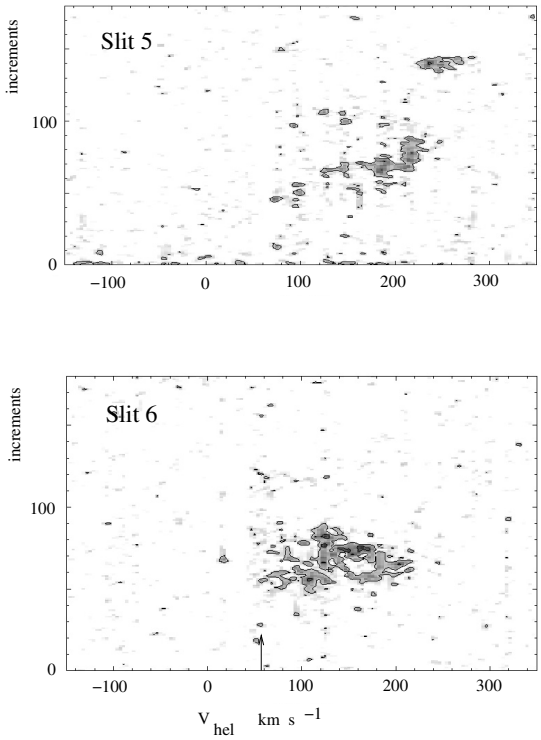

Fig. 4. As for Fig. 4 but for the northern knots covered by slit lengths 5 and 6.

The profiles have been smoothed by a Gaussian of 1.5 times the 20 km s^{-1} instrumental HPBW.

3. Discussion

3.1. The bipolar outflow

The radial velocities of the south stream of knots shown in Fig. 3 show a shift of around –150 km s^{-1} with respect to the heliocentric systemic radial velocity $V_{sys} = 56$ km s^{-1} as given by Matthews et al. (2008 – N.B. $V_{LSR} = V_{HEL} - 9.44$ km s^{-1} for Mira A). A very similar shift, but now to positive radial velocities, can be seen in Fig. 4 for the north stream on the opposite side of Mira A. Only the more distant arc from Mira A (Figs. 1 and 2) covered by the element Slit 5a (see the profile in Fig. 5) has a greater shift (200 km s^{-1}) in radial velocity with respect to V_{sys}. There therefore seems to be a strong bipolar structure to the principal elements of this outflow.

This expansion radial velocity measurement of the bipolar lobes has to be combined with measuring their expansion tangential velocity relative to Mira A to determine their actual expansion velocity. The expansion proper motions (PMs) of the knots relative to Mira A are then required for this purpose. Simple inspection of the Hα image in Fig. 1b and the FUV image in Fig. 1c reveal that the knots in Hα emission are ≈2″ closer to the reference star at the bottom of both frames than in the FUV emission. This could indicate the displacement caused by a high-expansion PM in the intervening 1.9 y between the two observations leading to an expansion velocity of ≈600 km s^{-1}. However, a more likely cause is the spatial difference within the knots of the Hα and FUV emission regions.

This suggestion is born out by the spatial displacement of Knot B (Fig. 2) in the first Palomar Observatory Sky Survey POSS I red plate taken on 26 Nov. 1954 and the Hα image in Fig. 1b obtained on 20 Oct. 2008. Only Knot B is clearly

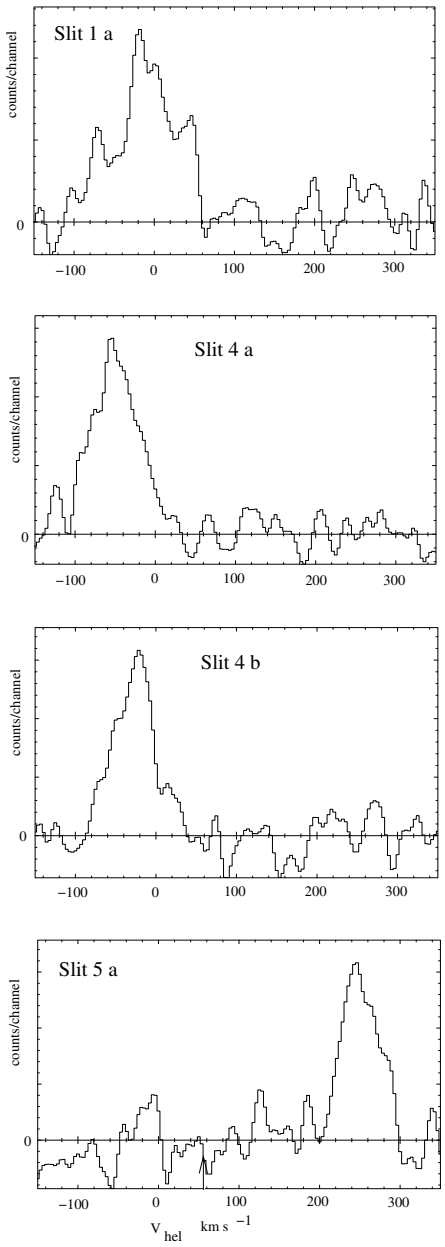

Fig. 5. Sample line profiles extracted from the pv arrays of line profiles in Figs. 3 and 4. That for Slit 1a is for Hα profiles from incremental lengths 30 to 50 coadded along Slit 1 in Fig. 3 and similarly profiles Slit 4a and b are for lengths 68 to 83 and 31 to 37 for Slit 4. The profile marked Slit 5a is for increments 132 to 144 along Slit 5 in Fig. 4. Again the heliocentric V_{sys} uses an arrow.

identifiable on this POSSI plate with the image of the brighter Knot A confused with that of a faint star.Curiously none of the Mira knots or this star was detected on the follow-up POSS II (23 Aug. 1995) red plate. However, using the STARLINK Gaia software the displacement of Knot B, measured with respect to the faint star field, in the intervening 53.90 y is +2″ in right ascension (α) and –17″ in declination (δ) with an uncertainty of ±2″ in both measurements determined mainly by the poor quality of the image of Knot B in the POSS I plate. This low quality is not surprising, because the POSS bandwidth is many times greater than the present one, and the photographic emulsion was the detector and the focal length shorter. The PM of Knot B is then measured as d(α, δ)/dt = (+37, –319) mas y^{-1}, each to around ±40 mas y^{-1} uncertainty. Here it is assumed that Hα dominates in the POSS I detection even though the bandwidth also encompasses the [S II] 6717 & 6731Å lines and much more continuum light than the present observations.

For comparison a similar PM measurement of Mira A itself was made between the POSS I and POSS II red plates. In the intervening 40.74 yr the displacement is –1.7″ in right ascension and -8.4″ in declination to give d(α, δ)/dt = (–40, –206) mas y^{-1} with (±30) mas y^{-1} uncertainties for the Mira A positions, because these were only determined from the centroids of the diffraction spikes in the two images but still corrected for the small differences in coordinates of the faint star field.

It is interesting that these PM measurements show Knot B to be moving along PA = 173° which is reasonably aligned with the bipolar axis of the south stream knots in Fig. 1 and tilted by a few degrees to the direction of Mira A (as noted by Martin et al. 2007) along PA ≈190°, which is also the orientation of the long FUV tail (Fig. 2). An expansion along this bipolar axis of ≈115 mas y^{-1} of Knot B relative to Mira A is therefore indicated to give an expansion tangential velocity of 58 ± 20 km s^{-1}. When combined with the expansion radial velocity of 150 km s^{-1}, this indicates an outflow velocity of ≈160 km s^{-1} tilted for the southern lobe at 69 ± 15° towards the observer with respect to the plane of the sky when all uncertainties are considered. More precise PM measurements of the knots are required to refine these estimations. The PM of Knot B with respect to Mira A, which is 127″ away from it, gives a time of ≈1000 y since its ejection. The Mira A outburst in 1070 (Ho 1962; Hoffleit 1997) then becomes a candidate for the creation of these bipolar lobes.

3.2. The leading bowshock

The preceding arc of FUV emission in Mira A's direction of motion has been interpreted as a bowshock being generated by the 120 km s^{-1} space motion of Mira A through the local ISM (Martin et al. 2007). It should now be considered that the bipolar outflow identified here could contribute to creating this bowshock. In either case the radial velocity measurements (Figs. 3 and 4) and the angular extent of the bipolar lobes (Fig. 1) certainly indicate, without consideration of expansion PMs, that the outflow velocity is ≈200 km s^{-1}. Incidently several planetary nebulae (PNe) with central binary systems, one star of which has evolved beyond its Mira A AGB phase, exhibit bowshock emitting optical lines, as they plough through the local ISM (Bond & Livio 1990, and refs. therein). However, if bipolar ejecta are favored as the creators of these bowshocks, then why has GALEX only detected one such system?

3.3. Evolution

Mira A is currently in its AGB phase showing all the signs of soon evolving into a complex PN, maybe with multiple bipolar lobes. For comparison, similar lobes of the PN NGC 6302 were conclusively shown to have been ejected at high velocity (630 km s^{-1}; Meaburn et al. 2005, 2008) and formed over a period of ≈2000 yr. The bipolar outflow from Mira A revealed here could easily develop into such features over a similar timescale. Meanwhile, if Mira A itself evolves into a hot PN progenitor while shedding its outer layers in its current AGB phase, these high speed lobes will become radiatively ionized during this period and emit a wide range of emission lines.

Acknowledgements. We acknowledge the excellent support of the staff at the San Pedro Martir observatory during these observations. JAL gratefully acknowledges financial support from DGAPA-UNAM grant IN116908. M.P.R. is supported by the IRCSET, Ireland. We are grateful to the referee, Dr. B. Welsh, for drawing our attention to the image of southern knots on the POSS I plates.

References

Bond, H. E., & Livio, M. 1990, ApJ, 355, 568
Boumis, P., Meaburn, J., Redman, M. P., & Mavromatakis, F. 2006, A&A, 457, L13
Ho, P. Y. 1962, VA, 5, 127
Hoffleit, D. 1997, J. Am. Ass. Var. Star. Observ., 25, 115
Ireland, M. J., Monnier, J. D., Tuthill, P. G., et al. 2007, ApJ, 662, 651
Karovska, M., Schiegel, E., Hack, W., Raymond, J. C., & Wood, B. E. A. 2005, ApJ, 623, L137
Martin, D. C., Seibert, M., Neill, J. D., et al. 2007, Nature, 448, 780
Karovska, M., Hack, W., Raymond, J., & Guinan, E. 1997, ApJ, 482, L175
Matthews, L. D., Libert, Y., Gérard, E., Le Bertre, T., & Reid, M. J. 2008, ApJ, 684, 603
Meaburn, J., Blundell, B., Carling, R., et al. 1984, MNRAS, 210, 463
Meaburn, J., López, J. A., & O'Connor, J. A. 1999, ApJ, 516, L29
Meaburn, J., López, J. A., Gutiérrez, L., et al. 2003, RMxAA, 39, 185
Meaburn, J., Boumis, P., Redman, M. P., López, J. A., & Mavromatakis, F. 2004, A&A, 422, 602
Meaburn, J., López, J. A., Steffen, W., Graham, M. F., & Holloway, A. J. 2005, AJ, 130, 2303.
Meaburn, J., Lloyd, M., Vayet, N. M. H., & López, J. A. 2008, MNRAS, 385, 269
Percy, J. R., & Bagby, D. H. 1999, PASP, 111, 203
Raga, A. C., & Cantó, J. 2008 ApJ, 685, L141
Reid, M. J., & Goldston, J. E. 2001, ApJ, 568, 931
Wareing, C. J., Zijlstra, A. A., O'Brien, T. J., & Seibert, M. 2007, ApJ, 670, L125